International Journal of Scientific Research and Engineering Development-– Volume 4 Issue 3, May-June 2021

Available at www.ijsred.com

RESEARCH ARTICLE OPEN ACCESS

Analysis and Simulation of LLC Resonant DC-DC Converter for Photovoltaic Applications

GeorgiPetrovTerziyski*

*(Department of Automation, Information and Control Engineering, University of Food Technologies – Plovdiv, Bulgaria
Email: georgi_terziyski@abv.bg)

----------**********----------

Abstract:

An analysis of LLC resonant DC-DC converters with a capacitive output filter has been performed, which will give information to the designer of resonant converters, what should be the type of LLC configuration, respectively the type of resonant circuit at a specific frequency detuning. Harmonic analysis was used for the theoretical study. As a result of the analysis, the expressions for the output and control characteristics of the considered configurations of converters are obtained. In addition, for some of the considered configurations, an output voltage higher than the supply voltage is obtained.

Keywords **—LLC resonant DC-DC converter, photovoltaic applications**

----------**********----------

I. INTRODUCTION

One of the most promising areas of modern energy are photovoltaic (solar) panels. They convert solar energy into voltage, which can be used either for personal consumption or for sale to energy distribution companies. These panels need to be as efficient as possible, which in turn leads to an increase in the efficiency of the resonant transducer used. Resonant converters have found extremely wide application in the construction of power supply devices for electric units for electric arc welding, lasers, fluorescent lamps and many others. The most commonly preferred resonant converters use three reactive elements in their resonant circuit, and they can operate in the entire range from idle to short circuit while maintaining the conditions for soft switching of the control switches in the inverter. Many authors [1] - [7] have considered LLC resonant transducers used in their connection to solar (photovoltaic) panels.

The aim of the present work is to perform an analysis of LLC resonant DC-DC converters on their obtained output and control characteristics, thus determining their advantages and disadvantages.

II. ANALYSIS OF THE CONVERTER

The diagram of the converter under consideration is shown in fig. 1. It consists of an inverter (controllable switches $S_1 \div S_4$with reverse diodes $D_1 \div D_4$), a resonant tank, a matchingtransformer(T_r), a capacitive filter (C_F),and a load resistor (R_0).

Different configurations composed of LLC resonant tanks, each of which has been studied for the converter under consideration, are shown in fig. 2 [8] – [9].

For the purposes of the analysis it is assumed that all the elements in the diagram are ideal (no losses in them), the power devices switch from one state into another instantly, the matching transformer has a coefficient of transformation equal to unity, and the pulsations of the supplying U_d and the output voltages $U_0$are negligibly small [10] –[11].

The following notations are accepted:

$U_0^{'} = U_0 / U_d$ - normalized output voltage;

$I_0^{'} = I_0 / (U_d / \rho_0)$ -normalizedoutputcurrent;

$R_0^{'} = R_0 / \rho_0 = U_0^{'} / I_0^{'}$ - normalizedload parameter;

$\rho_0 = \sqrt{L_1 / C}$ - wave resistance of the oscillating circuit;

$\nu = \omega_s / \omega_0$ -frequency distortion of the oscillating circuit;

ω_s - operational frequency of the converter;

$\omega_0 = 1/\sqrt{L_1 C}$ - resonant frequency of the oscillating circuit;

$a = L_2 / L_1$ - inductive's ratio between the two inductivities in the oscillating circuit.

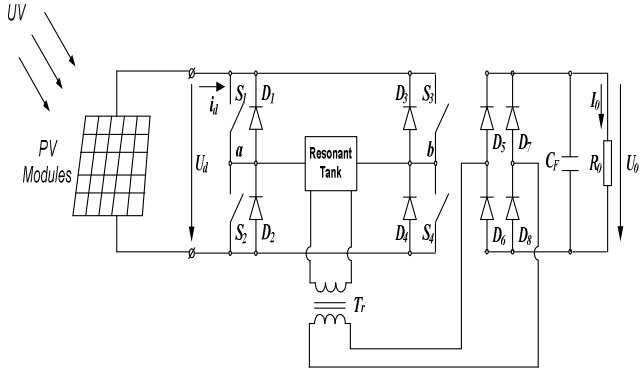

Fig.1. PV Module with a resonantDC-DCconverter with a capacitive output filter

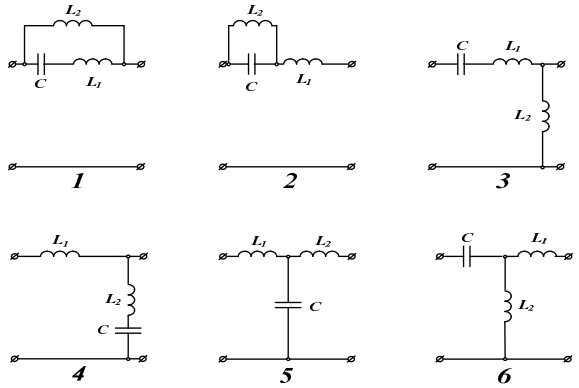

Fig.2. Configuration of LLCresonant tanks

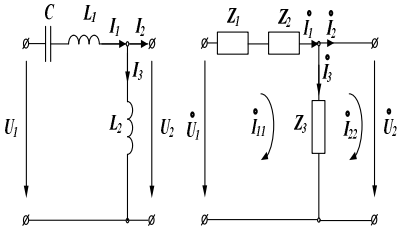

Fig. 3.Resonant tank

To show how the analysis is performed, we will consider a resonant circuit - configuration № 3 of Fig.2, which is the most common case of a resonant circuit in LLC resonant converters for photovoltaic applications.

For simplicity, we assume that the two circuits are equivalent, then, according to the contour current method, we compile the following system of equations:

$$\begin{cases} (Z_1 + Z_2 + Z_3)\dot{I}_{11} - Z_3.\dot{I}_{22} = \dot{U}_1 \\ -Z_3.\dot{I}_{11} + Z_3.\dot{I}_{22} = -\dot{U}_2 \end{cases} \quad (1)$$

After formal transformations, we express $\dot{U}_2$, i.e.

$$\dot{U}_2 = \frac{\dot{U}_1.Z_3 - Z_1 Z_3 \dot{I}_{22} - Z_2 Z_3 \dot{I}_{22}}{Z_1 + Z_2 + Z_3} \quad (2)$$

Let us replace the impedances of the coils and the capacitor from the resonant circuit with their equalities

$$Z_1 = 1/\, j\omega C = \rho_0 / j.\nu\,;$$

$$Z_2 = j\omega L_1 = j.\nu.\rho_0\,; \quad (3)$$

$$Z_3 = j\omega L_2 = a.Z_2 = j.\nu.\rho_0.a\,.$$

After substituting (3) into (2) and formal transformations we get:

$$\dot{U}_2 = \frac{\dot{U}_1.\nu^2.a}{\nu^2.a + \nu^2 - 1} + j\frac{\nu.\rho_0.a.(1-\nu^2).\dot{I}_{22}}{\nu^2.a + \nu^2 - 1} \quad (4)$$

The vector diagram of the voltages from the resonant circuit is as follows:

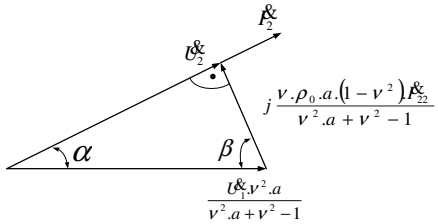

Fig. 3.Vector voltage diagram

For the obtained rectangular triangle the Pythagorean theorem is in effect:

$$\dot{U}_2^2 + \left[\frac{\nu.\rho_0.a.(1-\nu^2).\dot{I}_{22}}{\nu^2.a + \nu^2 - 1}\right]^2 = \left[\frac{\dot{U}_1.\nu^2.a}{\nu^2.a + \nu^2 - 1}\right]^2 \quad (5)$$

After formal transformations we get:

$$\dot{U}_2.(\nu^2.a + \nu^2 - 1)^2 + \nu^2.\rho_0^2.a^2.(\nu^2 - 1)^2.\dot{I}_{22} = \dot{U}_1.\nu^4.a^2 \quad (6)$$

where: $\dot{U}_1 = \frac{2.\sqrt{2}}{\pi}.U_d$

$$I_{22} = \frac{\pi}{2.\sqrt{2}}.I_0 \quad (7)$$

$$U_2 = \frac{2.\sqrt{2}}{\pi}.U_0$$

By substituting the dependencies (7) in (6) and formal transformations in relative units we get:

$$U_0' = \sqrt{\frac{\nu^4.a^2 - (\pi^4/64).\nu^2.a^2(\nu^2-1)^2.I_0'^2}{(\nu^2.a+\nu^2-1)^2}} \quad (8)$$

The last expression (8) gives the equation of the wanted output characteristics $U_0' = f(I_0', \nu, a)$.

The output power of the converter in relative units can be expressed from the equation for the output characteristics, after its multiplication by I_0' :

$$P_0' = \frac{I_0'}{8.(\nu^2.a+\nu^2-1)}\sqrt{64\nu^4.a^2 - \pi^4.\nu^2.a^2.(\nu^2-1)^2.I_0'^2} \quad (9)$$

With a set value of ν ,the function $P_0' = f(I_0', \nu, a)$ has a maximum at

$$U_0' = \frac{\nu^2.a}{\sqrt{2}.(\nu^2.a+\nu^2-1)} \text{ and } I_0' = \frac{4\sqrt{2}.\nu}{\pi^2.(\nu^2-1)} \quad (10)$$

$$P_{0\max}' = \frac{4.\nu^3.a}{\pi^2.(\nu^2.a+\nu^2-1).(\nu^2-1)} \quad (11)$$

The relative resistance of the resistor in which it is distributed the maximum power is:

$$R_{0\max}' = \frac{\pi^2.\nu.a(\nu^2-1)}{8.(\nu^2.a+\nu^2-1)} \quad (12)$$

III. CHARACTERISTICS OF LLC RESONANT CONFIGURATIONS

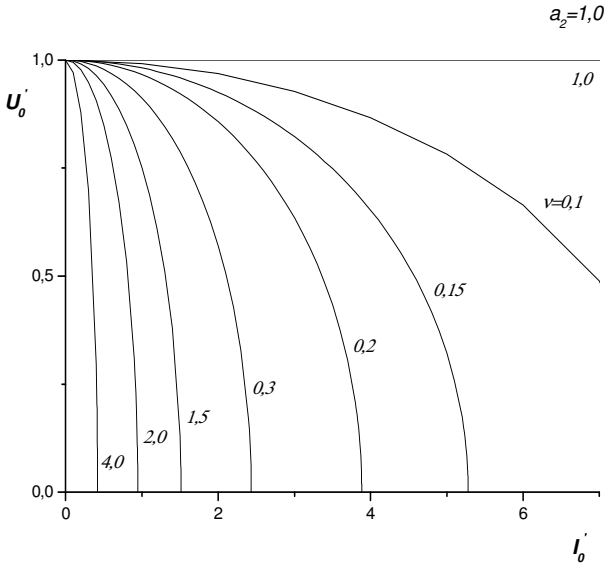

Fig.3. Output characteristics for configuration №1 from Fig.2

$$U_0' = \sqrt{\frac{(\nu^2.a_2+\nu^2-1)^2 - (\pi^4/64).(\nu.a_2-\nu^3.a_2)^2.I_0'^2}{(\nu^2.a_2+\nu^2-1)^2}} \quad (13)$$

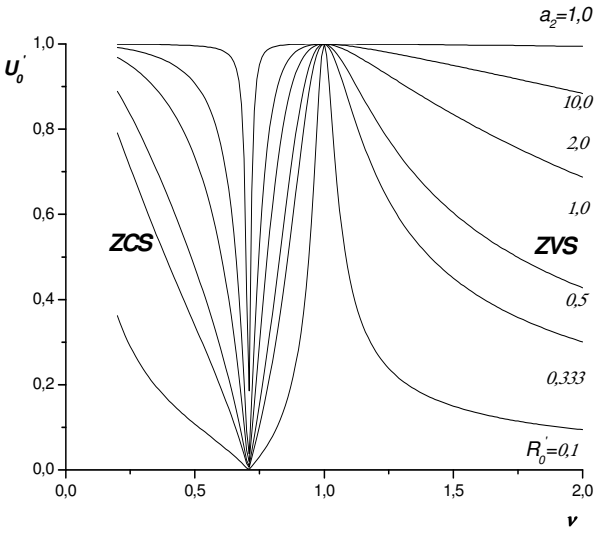

Fig.4. Control characteristics for configuration №1 from Fig.2

$$U_0' = \frac{8.R_0'.(\nu^2.a_2+\nu^2-1)}{\sqrt{64.R_0'^2.(\nu^2.a_2+\nu^2-1)^2 + \pi^4.(\nu.a_2-\nu^3.a_2)^2}} \quad (14)$$

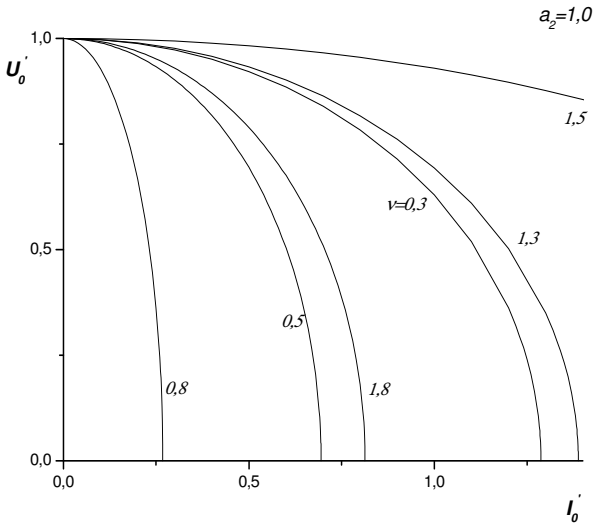

Fig.5. Output characteristics for configuration №2from Fig.2

$$U_0^{'}=\sqrt{\frac{(\nu^2.a_2-1)^2-(\pi^4/64).\nu^2.(1+a_2-\nu^2.a_2)^2.I_0^{'2}}{(\nu^2.a_2-1)^2}} \quad (15)$$

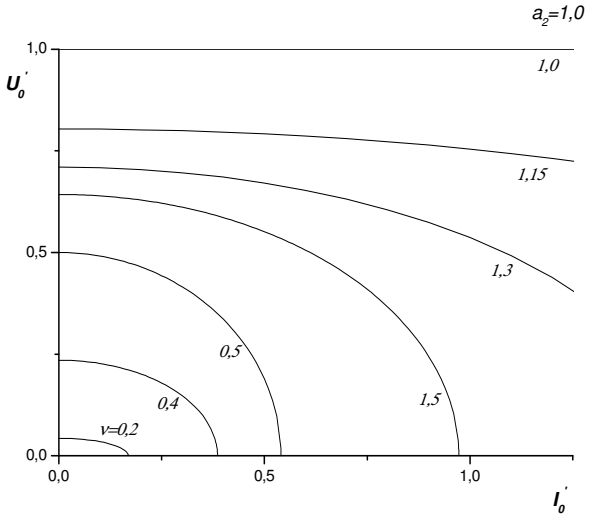

Fig.7. Output characteristics for configuration №3 from fig.2

$$U_0^{'}=\sqrt{\frac{\nu^4.a_2^{\,2}-(\pi^4/64).\nu^2.a_2^{\,2}.(\nu^2-1)^2.I_0^{'2}}{(\nu^2.a_2+\nu^2-1)^2}} \quad (17)$$

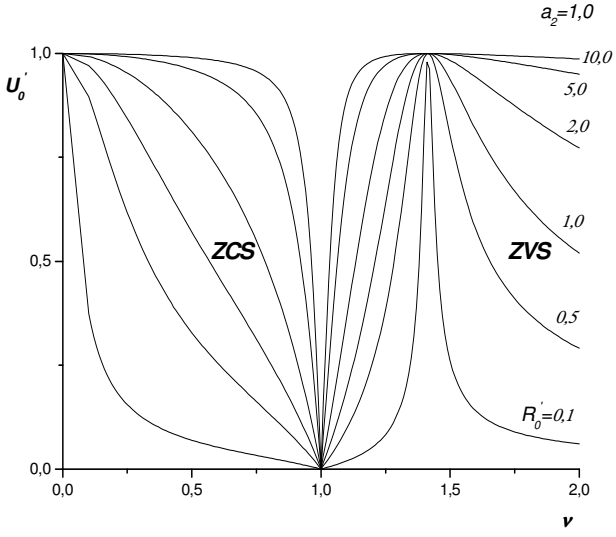

Fig.6. Control characteristics for configuration №2 from Fig.2

$$U_0^{'}=\frac{8.(\nu^2.a_2-1).R_0^{'}}{\sqrt{64.R_0^{'2}.(\nu^2.a_2-1)^2+\pi^4.\nu^2.(1+a_2-\nu^2.a_2)^2}} \quad (16)$$

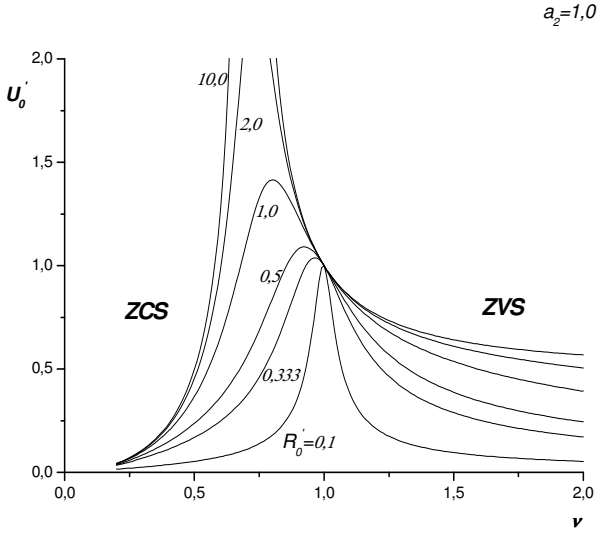

Fig.8. Control characteristics for configuration №3 from fig.2

$$U_0^{'}=\frac{8.\nu^2.a_2.R_0^{'}}{\sqrt{64.R_0^{'2}.(\nu^2.a_2+\nu^2-1)^2+\pi^4.\nu^2.a_2^{\,2}.(\nu^2-1)^2}} \quad (18)$$

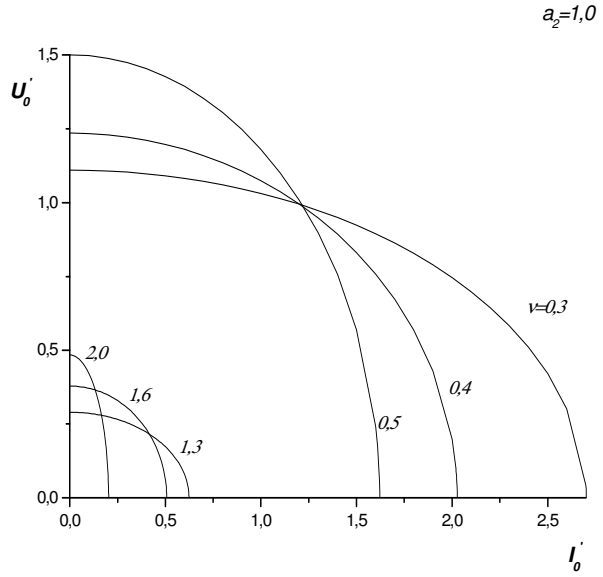

Fig.9. Output characteristics for configuration №4 from fig.2

$$U_0^{'} = \sqrt{\frac{[1-(\pi^4/64).\nu^2.a_2{}^2.I_0^{'2}].(\nu^2-1)^2}{(\nu^2.a_2+\nu^2-1)^2}} \qquad (19)$$

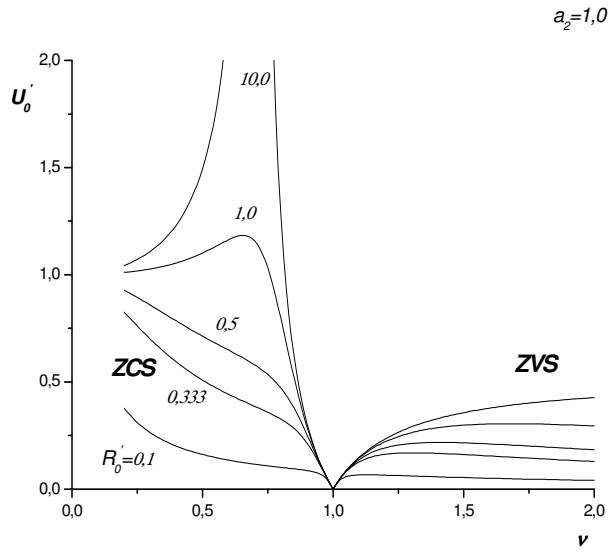

Fig.10. Control characteristics for configuration №4 from fig.2

$$U_0^{'} = \frac{R_0^{'}.(\nu^2-1)}{\sqrt{R_0^{'2}.(\nu^2.a_2+\nu^2-1)^2+(\pi^4/64).\nu^2.(\nu^2-1)^2.a_2{}^2}} \qquad (20)$$

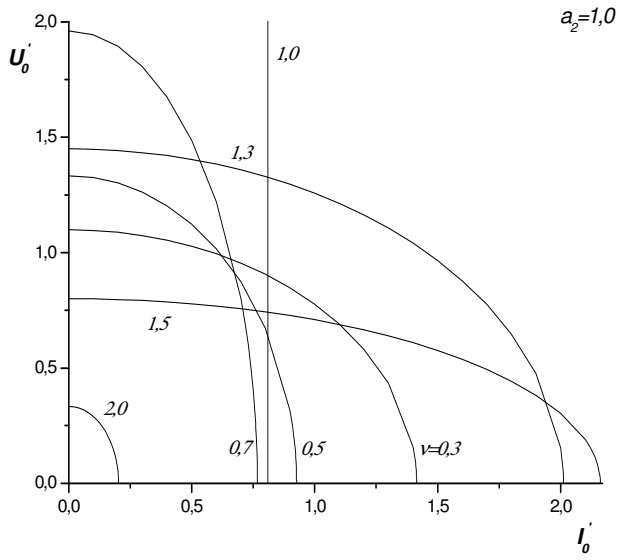

Fig.11. Output characteristics for configuration №5from fig.2

$$U_0^{'} = \sqrt{\frac{1-(\pi^4/64).[\nu.a_2.(\nu^2-1)-\nu]^2.I_0^{'2}}{(\nu^2-1)^2}} \qquad (21)$$

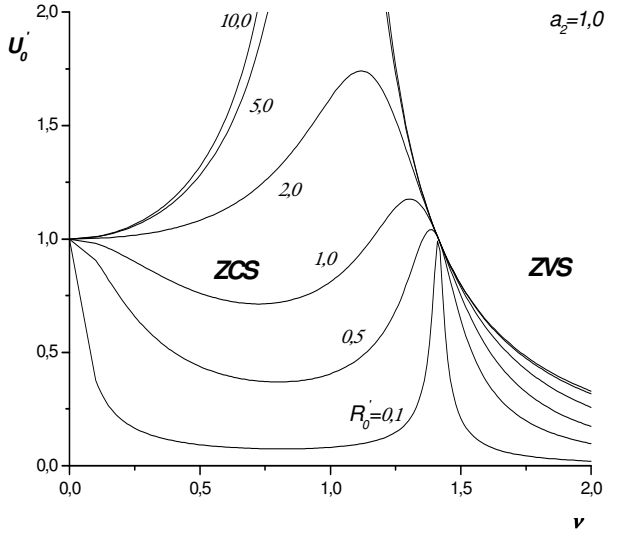

Fig.12. Control characteristics for configuration №5from fig.2

$$U_0^{'} = \frac{8.R_0^{'}}{\sqrt{64.R_0^{'2}.(\nu^2-1)^2+\pi^4.[\nu.a_2.(\nu^2-1)-\nu]^2}} \qquad (22)$$

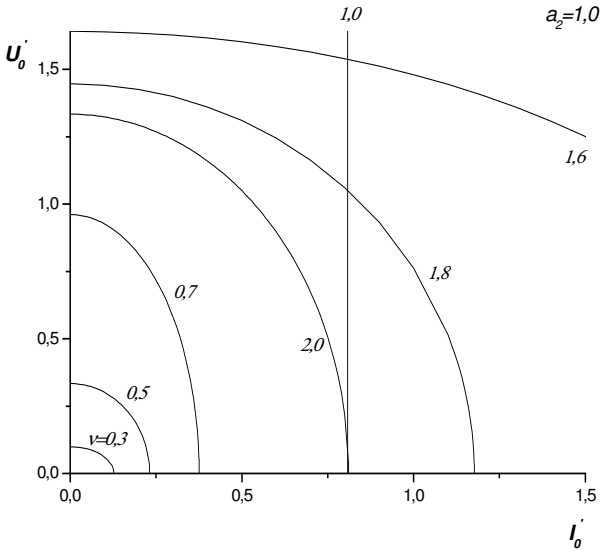

Fig.13. Output characteristics for configuration №6 from fig.2

$$U_0^{'} = \sqrt{\frac{\nu^4.a_2^{\ 2} - (\pi^4/64).\nu^2.(1+a_2-\nu^2.a_2)^2.I_0^{'2}}{(\nu^2.a_2-1)^2}} \quad (23)$$

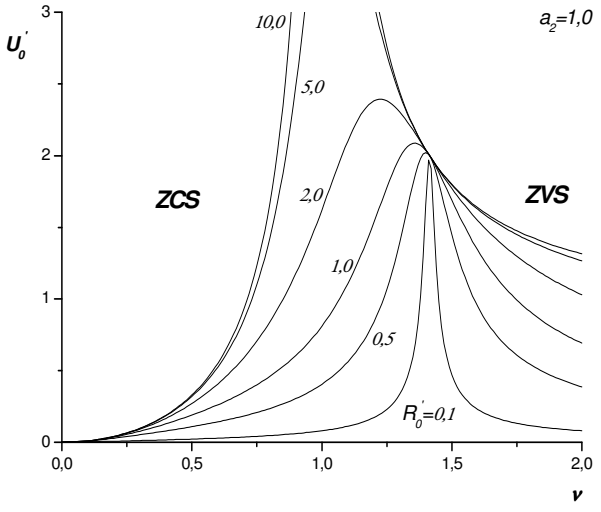

Fig.14. Control characteristics for configuration №6 from fig.2

$$U_0^{'} = \frac{8.\nu^2.a_2.R_0^{'}}{\sqrt{64.R_0^{'2}.(\nu^2.a_2-1)^2 + \pi^4.\nu^2.(1+a_2-\nu^2.a_2)^2}} \quad (24)$$

IV. Analysis of the Resulting Characteristics

The output characteristics given in Fig. 3 are arranged concentrically and show that when the converter is operating below and above its resonant frequency, with increasing operating frequency from $\nu = 0{,}1 \div 0{,}3$ and $\nu = 1{,}5 \div 4{,}0$, the short-circuit current decreases, but the no-load voltage remains constant. These are characteristics inherent in a current-limited voltage source.

The output characteristics given in Fig. 5 show that when the converter is operating below its resonant frequency, as the operating frequency increases from $\nu = 0{,}3 \div 0{,}8$, the short-circuit current decreases, but the no-load voltage remains constant. These are characteristics located concentrically and are inherent in a voltage source limited by current.

The output characteristics given in fig. 7 show that during operation of the converter for below its resonant frequency, with increasing operating frequency from $\nu = 0{,}2 \div 0{,}5$, the short-circuit current and the no-load voltage increase. These are concentrically located characteristics and are inherent in a current source that is resistant to operation and short circuit. When the converter is operating at above its resonant frequency, as the operating frequency increases from $\nu = 1{,}15 \div 1{,}5$, the short-circuit current and the no-load voltage decrease.

The output characteristics given in Fig. 9 show that when the converter is operating below its resonant frequency, with an increase in the operating frequency from $\nu = 0{,}3 \div 0{,}5$, the short-circuit current decreases, but the no-load voltage increases. These are characteristics that intersect and are inherent in a current-limited voltage source. When the converter is operating above its resonant frequency $\nu = 1{,}3 \div 2{,}0$, with increasing operating frequency, the short-circuit current decreases, but the no-load voltage increases. These are characteristics that also intersect and are inherent in a current-limited voltage source.

The output characteristics given in Fig. 13 show that when the converter is operating below its

resonant frequency, as the operating frequency increases from $\nu = 0{,}3 \div 0{,}7$, the short-circuit current and the no-load voltage increase. These are characteristics inherent in a current-resistant working and short-circuit current source. When the converter is operating at above its resonant frequency, with the increasing of the resonant frequency from $\nu = 1{,}6 \div 2{,}0$, the short-circuit current and the no-load voltage decrease.

It can be noted that all output characteristics are represented graphically by ellipse arcs, while all control characteristics have a clearly defined maximum, the value of which increases with increasing value of the load resistor.

The location of the maximum is shifted at the same time. It can also be noted that some of the obtained output and control characteristics are similar. From the graphs of the control characteristics it is obvious that some changes in the output voltage are achieved with a relatively small change in the operating frequency. Along with other control characteristics, the graphs show that with increasing value of $R_0^{'}$, the idle voltage and the operating frequency also increase.

V. Design of LLC Resonant DC-DC Converter

When designing the resonant DC-DC converter, the following parameters are usually set: output power P_0, output voltage U_0 and operating frequency f [11]. Assuming that the efficiency of the inverter is equal to one, the parameters of the power source are:

$$U_d = \frac{U_0}{U_0^{'}} = \frac{U_0}{\sqrt{\frac{\nu^4.a^2 - (\pi^4/64).\nu^2.a^2(\nu^2-1)^2.I_0^{'2}}{(\nu^2.a+\nu^2-1)^2}}} \quad (25)$$

$$I_d = \frac{P_0}{U_d} = \frac{P_0.\sqrt{\frac{\nu^4.a^2 - (\pi^4/64).\nu^2.a^2(\nu^2-1)^2.I_0^{'2}}{(\nu^2.a+\nu^2-1)^2}}}{U_0} \quad (26)$$

The values of the switching elements L_1, C and L_2 are determined by the expressions for the maximum output power and the distortion of the resonant circuit:

$$P_0 = \frac{4.\nu^3.a}{\pi^2.(\nu^2.a+\nu^2-1).(\nu^2-1)}.\frac{U_d^2}{\sqrt{L_1/C}} \quad (27)$$

$$\nu = 2.\pi.f.\sqrt{L_1.C} \quad (28)$$

Then for L_1, C and L_2 the dependencies are obtained:

$$L_1 = \frac{2.\nu^4.a}{\pi^3.(\nu^2.a+\nu^2-1).(\nu^2-1)}.\frac{U_d^2}{f.P_0} \quad (29)$$

$$C = \frac{\pi.(\nu^2.a+\nu^2-1).(\nu^2-1)}{8.\nu^2.a}.\frac{P_0}{f.U_d^2} \quad (30)$$

$$L_2 = a.L_1 = \frac{2.\nu^4.a^2}{\pi^3.(\nu^2.a+\nu^2-1).(\nu^2-1)}.\frac{U_d^2}{f.P_0} \quad (31)$$

Using the above methodology, the values of the most important parameters of the rated nominal mode of the proposed converter for photovoltaic applications have been calculated. The output data is as follows:

$P_0 = 15W$; $f = 50kHz$; $U_d = 17{,}5V$; $\nu = 1{,}3$.

The following parameter values were obtained:

$L_1 = L_2 = 45{,}808\mu H$; $C = 373{,}804nF$;

$U_0 = 8{,}575V$; $I_0 = 1{,}739A$; $R_0 = 4{,}931\Omega$.

Using the OrCADPSpice program, a computer simulation of the proposed converter was performed. In Fig. 7 shows the voltage circuits on the oscillating circuit, the current through the coil L1, the current through the coil L2, the voltage on the switching capacitor C and the voltage on the load resistor R0.

There is a very good match between the results obtained from the numerical solution and the computer simulation. For example, the voltage on the load resistor R0 obtained at the maximum photovoltaic power (see Figure 7) is calculated with a relative error:

$$\delta_{U_{R_0}} = \frac{8{,}575 - 8{,}931}{8{,}931}.100\% = -3{,}99\%.$$

The resulting -3,99 % relative error achieves a practical accuracy (error ± 5 %). Therefore, the proposed design methodology is suitable for engineering calculations.

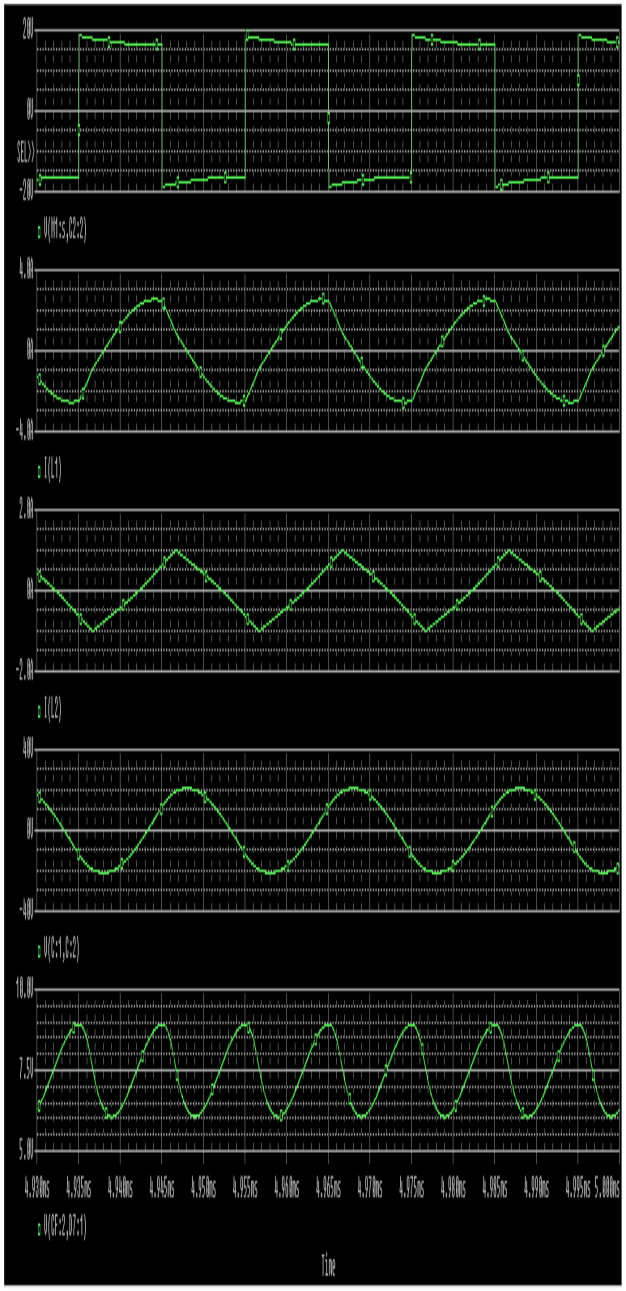

Fig. 7.Theresults of thecomputersimulation

Families of similar output and control characteristics shown in fig.2 are obtained for the configurations of LLC resonant circuits at $a=1,0$and at different values of the frequency distortion ν and the normalized load parameter $R_0^{'}$. The latter are shown in fig. 3-14. The equations of the output and control characteristics are given as well.

VI. CONCLUSION

Analysis of LLC resonant DC-DC converters with capacitive output filters has been carried out by the method of the first harmonic. Their operation below and above the operating frequency has been investigated. When their operating frequency is below the resonant one, the controllable switches switch at zero current (ZCS). On the contrary, when the operating frequency is higher than the resonant one, switching occurs at zero voltage (ZVS).

As a result from the analysis, equations of the output and control characteristics for a number of configurations of LLC resonant tanks have been obtained.Depending on the operation of the converter for below or above its resonant frequency, the obtained output characteristics show that the converter can operate as a voltage source or current source.

It has been established that the output voltage of the converter can have a higher value than the one of the supplying voltage. The results from this investigation could be applied to designing LLC converters used as supplying devices of electrical arc welding aggregates, luminescent lamps, lasers etc.

REFERENCES

[1] K. Rani, C. Rao, LLC Resonant Inverter for Solar PV Applications, IJAECS, Vol. 3, Issue 2, 2016, pp. 128 – 132.
[2] E. Eötvös, M. Bodor, DC/DC resonant converter for PV system, SCYR – 10th Scientific Conference of Young Researchers – FEI TU of Košice, 2010.
[3] L. Shivaraja, Modeling and Simulation of LLC Resonant Converter for Photovoltaic Systems, IJETIE, Vol. I, Issue 4, 2015, pp. 175 – 179.
[4] S. Sridhar, V. Naik, A ZVS Based Boost Resonant Converter for PV Applications, IEEJ, Vol. 7, No. 4, 2016, pp. 2212 – 2222.
[5] V. Thamaraimanalan, An Isolated Series Resonant Converter for PV Applications, IRJETM, Vol. 1, Issue 3, 2015, pp. 01 – 04.
[6] R. Seyezhai, G. Ramathilagam, P. Chitra and V. Vennila, Investigation of Half-Bridge LLC Resonant DC-DC Converter for Photovoltaic Applications, IJIREEICE, Vol. 1, Issue 3, 2013, pp. 76 – 81.
[7] C. Nagarajan, M. Muruganandam, D. Ramasubramanian, Analysis and Design of CLL Resonant Converter for Solar Panel-battery Systems, I.J. Intelligent Systems and Applications, 01, 2013, pp. 52 – 58.
[8] I. Batarseh, "Resonant Converter Topologies with Three and Four Energy Storage Elements", IEEE Transactions on Power Electronics, Vol. 9, No. 1, January 1994 pp. 64-73.
[9] B. Yang, Topology Investigation for Front End DC/DC Power Conversion for Distributed Power System, Dissertation, Virginia Polytechnic Institute, Blacksburg, 2003, pp. 247 – 307.
[10] N. Bankov, G. Terziyski, A. Vuchev and H. Dinkov, Analysis of serial-parallel resonant DC/DC Converter using the first harmonic method, Conference of Food Science, Engineering and Technologies, Vol. LVI, Issue 2, 2009, pp. 385 – 389 (in Bulgarian).
[11] N. Bankov, G. Terziyski, A. Vuchev and H. Dinkov, Work characteristics and design of serial-parallel resonant DC/DC Converter, Conference of Food Science, Engineering and Technologies, Vol. LVI, Issue 2, 2009, pp. 390 – 395 (in Bulgarian).

